Mixed Pluronic/Vitamin E conjugates self-assemblies for glipizide drug for antidiabetic evaluations

6.1: Introduction

Due to non-invasiveness, compliance, and convenience of administration, the oral route has been the most usable route of drug administration for the treatment of many diseases. But it has been well counted that almost 50% to 70% of the bioactive new drug compounds discovered recently by the pharma industry are lipophilic compounds, which limit oral routes to ensure better therapeutic efficacy [1]. The low aqueous solubility of these developed drug compounds also complicate the effects of the delivery of many existing applied drugs [2,3]. Hence, such lipophilic drugs have bioavailability problems correlated with solubility and dissolution in aqueous media [4]. The oral absorption of such lipophilic compounds has a typical dissolution rate that is directly proportional to aqueous solubility of the drug. Currently, the majority of the crystalline drugs under development are classified as BCS class-II (70%) and BCS class-IV (20%), while actual marketed drugs of 30% and 10% are classified as BCS class-II and BCS class-IV, respectively [5,6]. Therefore, to improve the dissolution rate and scope of oral absorption of important BCS class-II drugs, formulations based on nanotechnology like solid-lipid nanoparticles, microemulsions, liposomes, polymeric micelles etc. extend a better option for the oral route of drug delivery. Not only that, nanotechnology-based formulations are providing good stability, longer corneal contact times, excellent solubility, and a well-controlled drug release compared to conventional formulations [7–9].

Among these nanotechnology-based formulations, researchers have been drawn to the concept of polymeric micelles as better self-assemblies for the solubility and delivery of many useful lipophilic drugs [10]. Several ABCs have been employed to fabricate the polymeric micelles, of which Pluronic polymers have attracted a lot of attention because many of them are listed in the US as well as British Pharmacopoeia in the form of pharma excipients and are widely applied in a variety of medicinal uses. Pluronics are tri-block copolymers of PEO-PPO-PEO polymers [11]. Pluronic micelles have appeared as one of the most promising nanovehicles for the oral delivery of lipophilic and/or poor permeability based drugs [12,13] Pluronic micelles consist of a core-shell structure and have received notable attention because of nano in micelle size, high drug encapsulating, better stability, improved cellular uptake, and enhanced therapeutic potential [14,15]. The hydrophobic PPO

core can work as depot for lipophilic drugs, while the hydrophilic outer PEO shell offers steric effects of stabilization, promising the stability of micelles in water while holding a good amount of drug molecules [16]. Generally, the relative chain length of both PPO and PEO blocks in Pluronic determines their size and morphology. It may be spherical or cylindrical or lamellar in the media [17,18].

In the series of Pluronics, Pluronic®F127 is very effectively utilized as micellar nanovehicles because of its good biodegradability (FDA approved), biocompatibility, and outstanding mucus-penetrating property [19,20]. It has been used to improve the drug encapsulation efficiency, enhance the micellar stability, and prolong the circulation time for many drugs [21].

Mixed polymeric micelles of Pluronic F127 with TPGS have also shown potency as nanovehicles for the oral delivery of many lipophilic drugs [22–25]. TPGS is water-soluble vitamin E derivative and made by esterification of polyethylene glycol (PEG-1000) with vitamin E succinate. It showed notable surface adsorption and a significant impact on lipid model membrane, and its many properties make it viable in drug delivery formulations, including P-gp inhibition activity, solubilizing hydrophobic drugs, and enhancing drug permeation/penetration through the skin as well as intestinal walls [26–28]. The F127 and TPGS are both FDA-approved polymers that are highly safe for use in a wide range of drug formulations [25]. Mixed F127:TPGS micelles display synergistic properties, such as enhanced micelle stability and drug-incorporating efficiency, better than the individual substances, and have been identified as prospective nanovehicles for enhancing the oral bioavailability of lipophilic drugs [16,29].

A major issue come out with F127 is the high CMC values in between the range of 0.26 to 0.8 wt% [30,31], which take place the dissociation of nano-assemblies upon dilution in the liquid stream. The dissociation of nano-assemblies or micelles leads to the fast release of the drug before it gets the targeted action site. To overcome this problem associated with F127, several approaches have been investigated, including mixed micelles as well as structural modifications of it [32]. In this case, the structural modification of F127 with other biocompatible molecules resulted in many promising outcomes [33]. In this context, we created stearic acid-conjugated F127 (SA-F127) to replace F127 in the development of mixed micelles. The synthesized SA-F127 was well characterized using FTIR, ^{1}H-NMR, and GPC

measurements. The CMC of this synthesized SA-F127 was also measured using a pyrene probe technique.

The drug on which we are focusing is glipizide (GLN). GLN (Hypoglycemic agent, oral, BCS class-II) is prescribed for the cure and treatment of non-insulin-dependent diabetes patients [34,35]. It is an acidic drug with a low pKa (pKa = 5.9) that is generally insoluble in water and acidic environments [36]. When it is supplied orally, its absorption is inconsistent in the patients (diabetic), due to the weak gastric transportability and/or gastric emptying. Such inconsistent absorption of GLN is pharmacologically relevant, as its efficacy is absorption rate dependent [37]. Also, GLN absorption from the gastrointestinal(GI) fluids is limited due to its poor aqueous solubility [38]. In general, the dissolution of GLN at an *in situ* pH of 6.8 is highly recommended, but dissolution studies at such high pH may not be counted bio-relevant. Also, at high blood glucose level situations, GLN should display very high oral bioavailability. Therefore, the improvement of the aqueous solubility and dissolution rate of GLN is well in demand, irrespective of its use at a specific pH, for better pharma applications [39].

In this concern, in the present study, we developed a mixed polymeric micellar system composed of SA-F127 and TPGS, coded as GLN-PMM, as nanovehicles to overcome the major challenges of GLN's poor aqueous solubility and oral bioavailability. The GLN-PMM was fabricated by the thin-film technique. Using quality by design, the fabrication of GLN-PMM was optimized through a central composite design (CCD) model. The particle size, zeta potential, morphology, drug loading(%DL) and encapsulation efficiency(%EE), bio-compatibility, and solid crystallinity nature of the fabricated GLN-PMM were determined using advanced DLS, Zeta, TEM, SANS, FTIR, DSC, and XRD methods. The location of GLN drug in the GLN-PPM mixed micelles was confirmed through the ^{1}H-NMR technique. To understand the pharmacological activities, the mixed polymeric micellar formulations were also tested *in-vitro* for drug release studies, *ex-vivo* permeation study investigations, and *in-vivo* anti-diabetic study.

6.2: Experimental Section

6.2.1: Methods

6.2.1.1 Synthesis of SA-F127

Without the use of a solvent or a catalyst, SA was simply conjugated to Pluronic F127 during the molten state via esterification between the -COOH group(part of SA) and the -OH group(part of F127) [40]. In a 25-mL round-bottom flask, 5 g SA and 5 g F127 were taken and heated with constant stirring (250 rpm) to obtain a homogeneous molten liquid. They reacted at 150 °C–160 °C for 6 hrs. The resultant solution was dropped into ethyl acetate (EA)/petroleum ether (v/v) 1:1 mixture solution to separate the unreacted SA by filtration, which was not soluble in the reaction content. Finally, the synthesized SA-F127 was dried at RT in a vacuum oven under reduced pressure for 24 hrs. After purification, the product was confirmed using spectral techniques.

6.2.1.2 Experimental Design

GLN-PMM systems were constructed according to a two-factor central-composite-design (CCD) model using Design-Expert® software (Ver 7.0, Stat Ease, Inc., Minneapolis, USA) to examine the influence of the different responses on the mixed micellar parameters. The independent factors were the SA-F127 to GLN ratio (A) and the concentration of TPGS (%w/v) (B). The particle size, PDI, drug loading (% DL), and encapsulation efficiency (% EE) were selected as dependent responses. The lowest and highest levels of factor and response and their desirability constraints are tabulated in Table 6.1**.** The composition of the 13 formulations obtained through CCD (noted in standard order) is given in the Table 6.2**.** The significance of the model and term was determined using the ANOVA (Assessment of Variance) approach.

Table 6.1: CCD parameters for optimization of GLN-PMM system.

Factors	**Lower value (Coded as -1)**	**Upper value (Coded as +1)**
X1:Pluronic : drug ratio	10:1	40:1
X2:Percentage of TPGS (%w/v)	0.0	2.0
Responses		**Goal**
Y1: Particle size (nm)		Minimize
Y2: PDI		Minimize
Y3: %DL		Maximum
Y4: % EE		Maximum

Table 6.2: Experimental runs and results based on CCD.

No.	A:SA-F127 to drug ratio	B:TPGS (wt%)	Particle Size (nm)	PDI	% DL	%EE
1	10.00	0.00	175.1	0.4000	8.644	12.30
2	25.00	1.00	19.81	0.5060	1.092	67.96
3	40.00	1.00	43.18	1.000	3.494	71.52
4	40.00	2.00	53.28	1.000	2.099	96.60
5	25.00	1.00	19.18	0.5060	1.092	67.96
6	40.00	0.00	68.93	1.000	5.431	55.81
7	25.00	1.00	19.81	0.5060	1.092	67.96
8	10.00	1.00	60.28	0.3330	5.481	32.64
9	25.00	0.00	109.7	0.5800	3.475	39.78
10	25.00	1.00	19.03	0.5460	1.092	67.96
11	25.00	2.00	16.10	0.3180	0.616	78.26
12	10.00	2.00	14.13	0.2230	2.866	48.92
13	25.00	1.00	19.03	0.5060	1.092	67.96

6.2.1.3 Fabrication of GLN-PMM

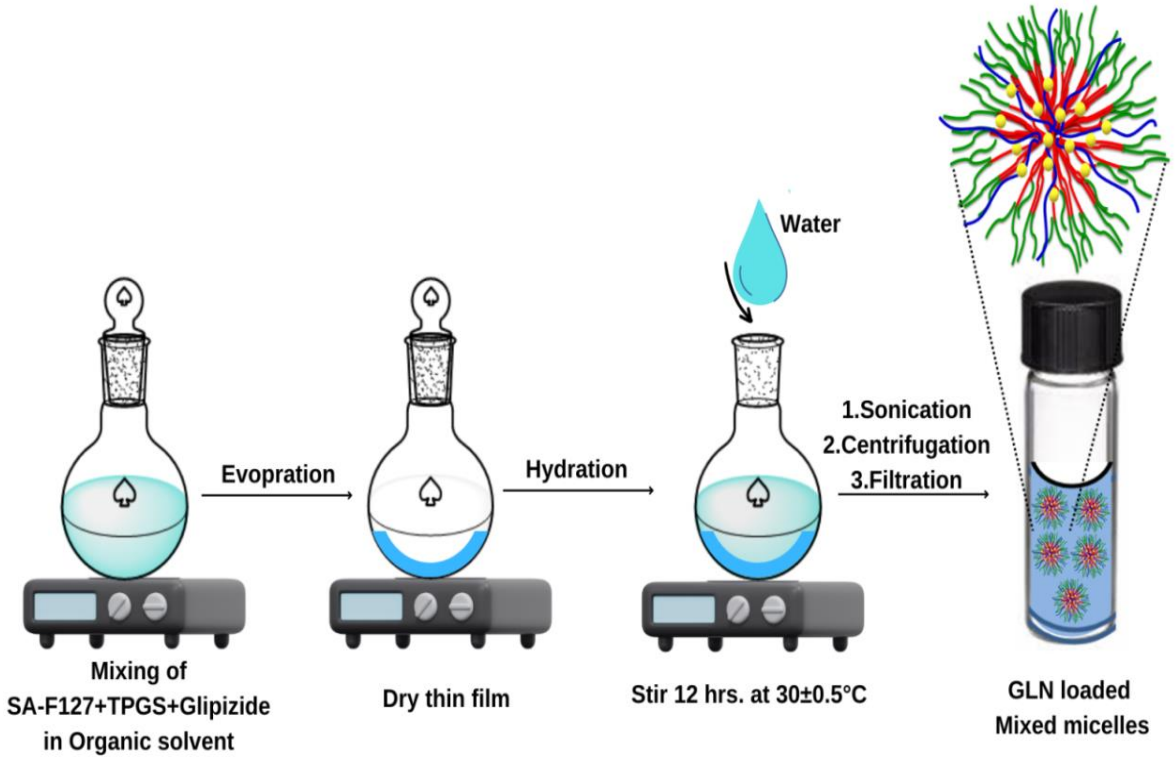

Scheme 1: Schematic illustration of the fabrication of GLN-PMM micellar system

The thin-film hydration technique was utilized to develop the PMM according to the proposed experimental design. The required amounts of SA-F127 and TPGS were dissolved in chloroform solvent in a RBF to get homogenized solutions. To obtain a thin, dry film, the solvent was evaporated slowly in a rotavapour at 60°±0.5°C. The dry thin film was then rehydrated with ultrapure water, sonicated for 15 minutes, and properly filtered through a nylon filter to obtain a PMM dispersion solution. For the GLN-PMM system, a predetermined amount of GLN (5 mg) was added to the previously prepared PMM solution, and the rest of the process was repeated (shown in Scheme 1). Further, the PMM and GLN-PMM systems are lyophilized under vacuum for 48 hours and stored at 2°-4°C.

6.2.1.4 Formulation optimization

The Design Expert® software produced the optimal GLN-PMM by imposing limits on the partical size, PDI, %DL, and %EE, as shown in Table 6.1. To verify the authenticity of the optimal formulation factors and estimated responses provided by the program, the suggested optimal GLN-PMM system was then prepared and studied.

6.2.2 Characterization methods

CMCs of SA-F127 and optimized mixed SA-F127:TPGS micelles were determined by pyrene probe method using fluorescence method. The solubility of GLN in the 1.0 %w/v micellar solutions of F127, TPGS, F127:TPGS, and SA-F127:TPGS was determined using UV-Vis spectroscopy. Mixed micellar size, zeta potential, morphological investigations and viscosity of optimized PMM and GLN-PMM were characterized using DLS, TEM, SANS and rheometer. CUR compatibility and stability in mixed micellar formulation investigated using FTIR, XRD, DSC and DLS techniques. The location of GLN in the GLN-PMM mixed micellar system was confirmed using ^{1}H NMR technique. The detailed procedure of the all-mentioned techniques is shown in Chapter 2.

6.2.3. Biological Investigations

6.2.3.1 In-vitro drug release and kinetic study

The *in-vitro* GLN release from the GLN-PMM system was investigated by a dialysis bag diffusion method. After membrane activation, it was filled with the GLN-PMM solution, which forms the donor compartment. For the receiver compartment, 0.1 N HCl (pH 1.2), 6.8 intestinal pH, and 7.4 blood pH were used, along with 0.37% Tween-20 and 10% DMSO as

the release medium. The dialysis bag was placed into the beaker, which contains receiver chamber fluid at the constant 37°±0.5°C temperature and stirred for 250±10 rpm. Samples were withdrawn at a fixed, pre-determined time interval and replenished with fresh release media at the same time. The amount of GLN release in the medium was quantified using UV-VIS spectroscopy. Also, the drug release data were fit to the different kinetic models in order to more detail about how GLN is released.

6.2.3.2 Ex-vivo permeation study

Ex-vivo drug permeability studies were done by Franz diffusion cell using isolated goat intestine segments. Fresh goat intestine was procured from a nearby slaughter house and stored in PBS of pH 6.8. It was then rinsed and cleansed using the Krebs-Ringer phosphate buffer solution. The experiment lasted 24 hours. The intestine segment was securely implanted between the donor and receptor chambers, with the intestine's inner lumen facing the donor chamber. The receptor chamber was made full with PBS. The assembly was continuously stirred at 120±10 rpm. In the donor chambers, 1.0 ml of the GLN-PMM solution was added. Aliquots were withdrawn from the receptor chambers at predefined time intervals, and the equivalent volume of fresh media was utilized to replace it. Here, the samples were analyzed at a λ of 275 nm using UV-Vis Spectrometer. The % diffusion of the GLN was quantified and graphically shown. The same approach was used to conduct the study with a pure GLN.

6.2.3.3 In-vivo anti-diabetic study

Normal male Wistar rats of 230–260 g in weight were kept in polypropylene cages in a room with controlled humidity and temperature and maintained conditioned with light-dark cycle for 12 hrs. The Institutional Animal Ethical Committee, Uka Tarsadia University, Gujarat, India (No:-MPC/IAEC/19/2021) examined and accepted the experimental protocol. All animals will be handled with follow all rule and regulations of CPCSEA. The rats were haphazardly arranged into 3 groups (n = 6) of each: Group I: diabetic control, Group II: marketed formulation, and Group III: GLN-PMM system. Before the beginning of the experiment, animals were fasted for 12 hours. A diabetic control (group 1) blood sample was collected from the tail vein of rats after induction of diabetes in all three groups. A reduced blood glucose level was estimated for both control and test samples. The marketer formulation and optimal GLN-PMM system were administered orally to each group using

stomach intubations. A GLN dose of 2.5 mg/kg, p.o. was administered. 1 mL of blood samples were collected at a pre-decided time point at 1, 2, 3, 4, 5, 6, 7, 8, 9, 10, and 24 hrs. The glucose level of the blood was determined by using an Accu-Chek glucometer. The statistical analysis is done using GraphPad Prism software. The results are presented as a mean ± standard deviation (SD).

6.3: RESULTS AND DISCUSSION

6.3.1 Characterization of SA-F127

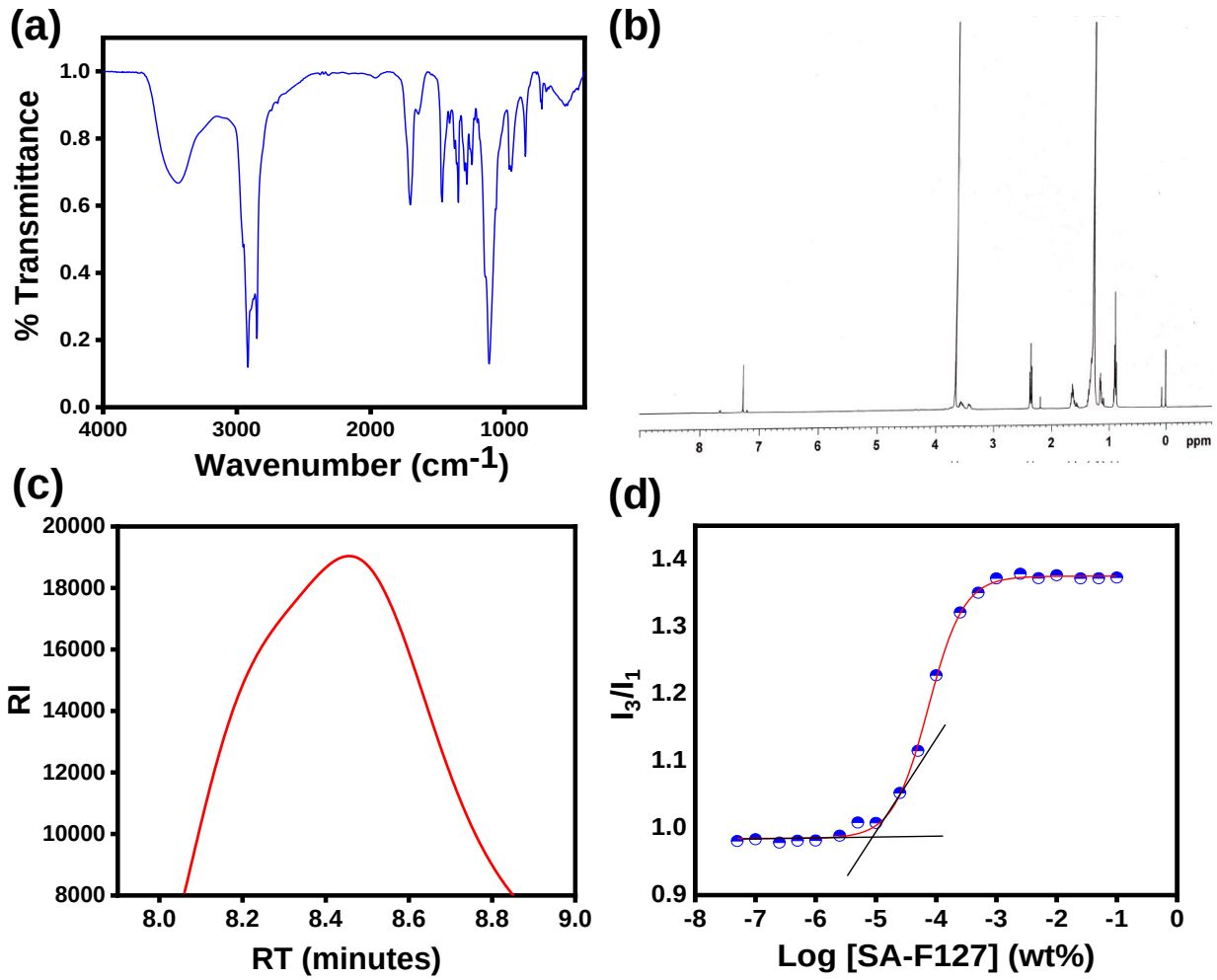

Figure 6.1: (a) FTIR Spectrum, **(b)** ^{1}H NMR Spectrum, **(c)** GPC profile, and (d) Plot I_3/I_1 versus logarithmic polymer concentration of the synthesized SA-F127.

The synthesized SA-F127 structure was characterized through FTIR, ^{1}H NMR and GPC. Also, its CMC was evaluated to confirm the surfactant structure behavior. The band around 1710.80 cm^{-1} of stretching vibration of C=O bonds of ester formation has been clearly seen in the FTIR spectra of SA-F127 (Figure 6.1(a)). The NMR spectrum of SA-F127 in $CDCl_3$ showed the δ of CH_2-O in PEO, CH_2-CH_2-O in PEO, -CH_2, -CH and –CH_3 of PPO,

at 3.66-3.64 ppm, 2.37-2.34 ppm, 3.42-3.39 ppm, 3.58-3.54 ppm and 1.314-1.267 ppm, respectively. While -CH_2 and -CH_3 of stearic acid in SA-F127 showed the δ at 1.661-1.625 ppm and 0.908-0.877 ppm, respectively (Figure 6.1(b)). The molecular weight of SA-F127 is 13293 $g.mol^{-1}$ confirmed by GPC, which found higher than the molecular weight of F127 (Figure 6.1(c)). The results of FTIR, ^1H NMR, and GPC was confirmed the successful conjugation of SA with F127. The CMC of the SA-F127 was measured using pyrene probe method is 8.6638 x 10^{-6} wt% (shown in Figure 6.1(d)) which one found better than the previously reported value [40]. Such low CMC of the SA-F127 is justified the better surfactant behavior of the synthesized polymer.

6.3.2 Solubility studies

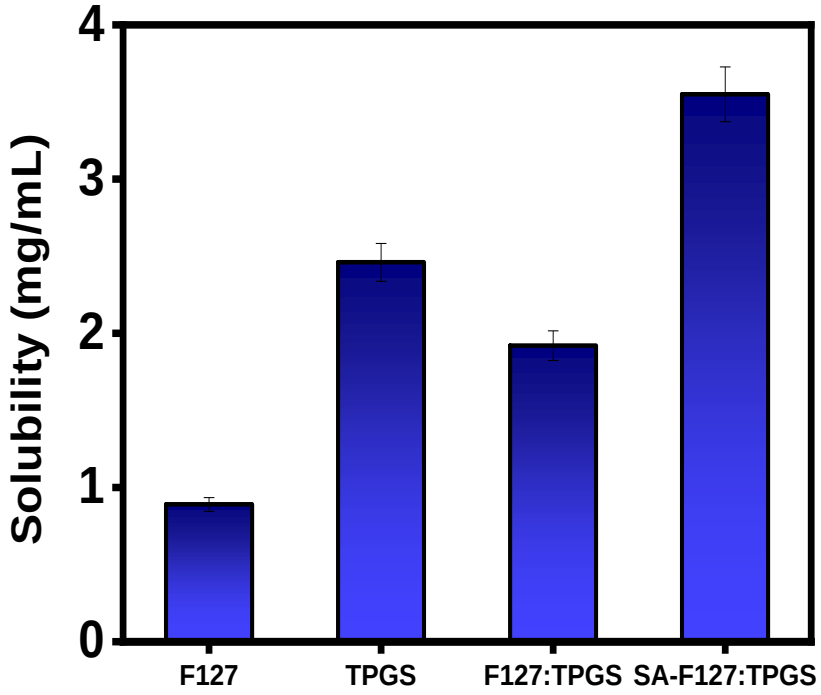

Figure 6.2: GLN solubility in the fixed 1.0 %w/v concentrations of F127, TPGS, mixed F127:TPGS, and mixed SA-F127:TPGS micellar solutions.

The solubility of GLN in the 1.0 %w/v micellar solutions of F127, TPGS, F127:TPGS, and SA-F127:TPGS was determined and presented in Figure 6.2. The solubility of GLN in the SA-F127:TPGS mixed micellar system is increasing as compared to F127, TPGS, and F127:TPGS mixed systems. In quantitative terms, the mixed SA-F127:TPGS micellar solution shows a sharp enhancement in GLN solubility from a water solubility of

0.0335±0.0021 mg/mL to 3.55 mg/mL [41]. As a result, the system composed of SA-F127 and TPGS was found to be suitable for the fabrication of the mixed micellar formulation for GLN drug and to be better for studying GLN bioavailability.

6.3.3 Optimization through CCD

In general, adequate precision provides the ability of model to navigate the CCD design. Here signal-to-noise ratios were observed >4 for all the responses justify the design. Additionally, the difference between the adjusted R^2 and the predicted R^2 shouldn't be greater than 0.2; otherwise, there may be an issue with the data or the model. For all responses in this design, adjusted and predicted R^2 were in considerable agreement.

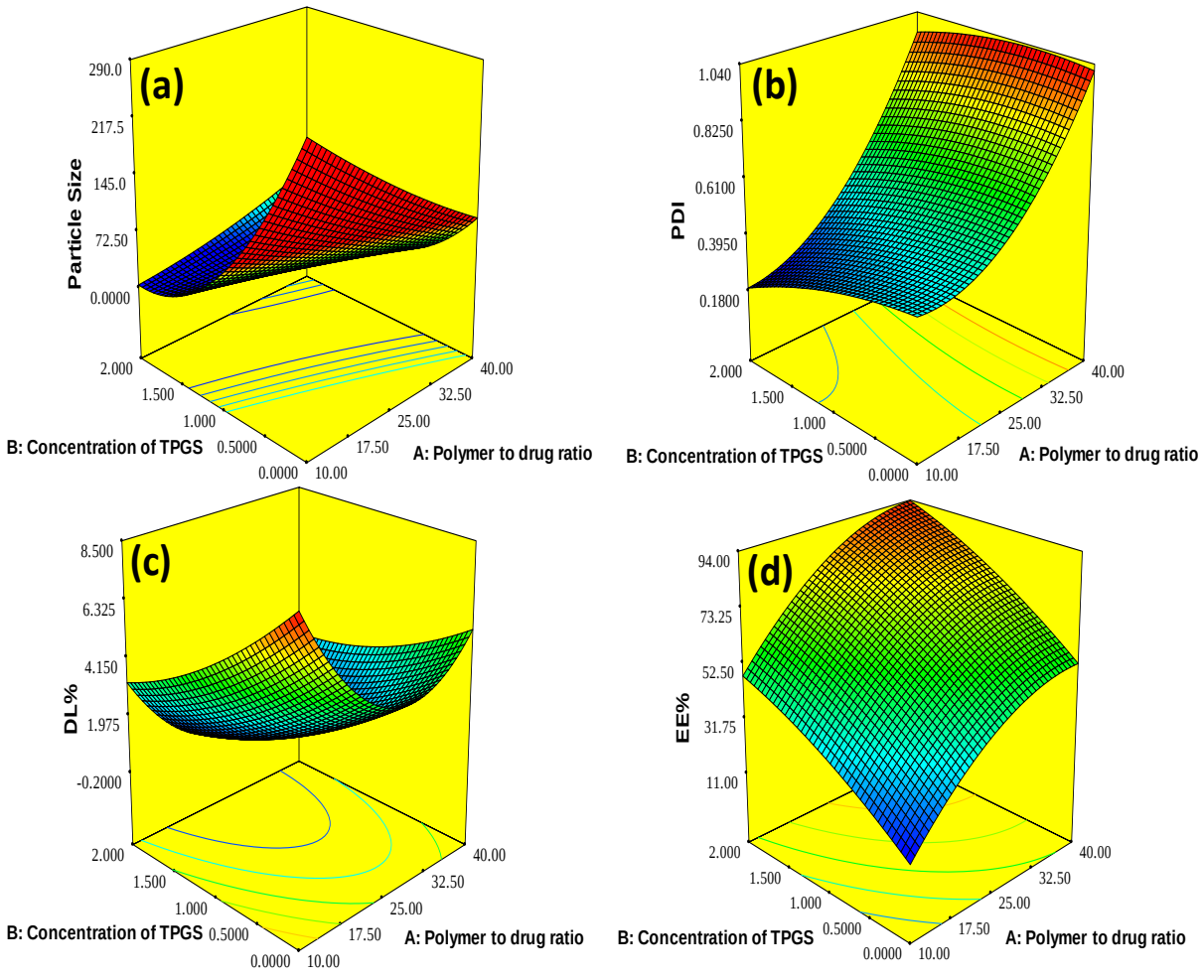

Figure 6.3: 3D response surface graphs for the effect of significant variable on **(**a**)** Particle Size, **(**b**)** PDI, **(**c**)** %DL, and (d) %EE.

6.3.3.1 The effect of studied variable on particle size of GLN-PMM system

Table 6.3 shows the summary statistics for particle size models. Data clearly showed the higher adjusted and prediction R^2 by the quadratic model and therefore allowing it the model of selection for particle size.

The following quadratic regression 2nd order equation of the well-fitted model was used to minimize particle size.

$$\text{Particle Size} = 21.77 - 14.02 \times A - 45.04 \times B + 36.33 \times AB + 23.96 \times A^2 + 35.13\ B^2 \ldots\ldots\ldots\ldots (1)$$

ANOVA analysis indicates that the SA-F127-to-GLN ratio and the concentration of TPGS had a notable influence on size of the micellar formulations. Increasing both parameters resulted in a significant reduction in particle size. Figure 6.3(a) depicts a 3D surface plot for the influence of the SA-F127-to-GLN ratio and concentration of TPGS on particle size. Decreasing the SA-F127-to-GLN ratio and enhancing the drug concentration relative to the SA-F127 may enhance the particle size due to the expansion of the micellar core region caused by the encapsulation of a high amount of GLN drug in a lower proportion of SA-F127 micelles [42]. Furthermore, increasing the drug concentration may cause drug molecules to adsorb to PEO shell of the micelles, resulting in particle size expansion [43].

6.3.3.2 The effect of studied variable on PDI of GLN-PMM system

Usually, polydispersity is used to indicate a distribution's level of non-uniformity of micelles. Regarding the PDI, a zero value demonstrates mono-dispersed particles and the value of 1 considers highly poly-dispersed particle [44]. The following quadratic regression 2nd order equation of the fitted model was utilized to minimize PDI:

$$\text{PDI} = 0.5065 + 0.3407 \times A - 0.0731 \times B + 0.0442 \times AB + 0.1787 \times A^2 - 0.0388 \times B^2 \ldots\ldots\ldots\ldots (2)$$

Here, the ANOVA analysis shows a significant effect on PDI with the changes in SA-F127-to-GLN ratio and TPGS concentration. According to the PDI model summary data in Table 6.3, the quadratic model obtained the higher adjusted R^2 and predicted R^2. Figure 6.3(b) depicts a 3D surface plot for the influence of SA-F127 to drug ratio and concentration of TPGS on PDI. The negative coefficient of B indicates that PDI significantly decreases with increasing levels of SA-F127-to-GLN ratio. The moderate PDI values demonstrated that the polymeric micellar system shows the well homogeneity in the dispersion.

6.3.3.3 The effect of studied variable on %DL of GLN-PMM system

The %DL of polymeric micelles can be applied as basic indicators of the interaction between the polymeric mixtures and drugs. The following 2nd order regression equation of the fitted quadratic model was used to maximize %DL.

$$\%DL = 1.186 - 0.9945 \times A - 1.995 \times B + 0.6114 \times AB + 3.067 \times A^2 - 0.6247 \times B^2 \quad \ldots\ldots(3)$$

ANOVA analysis clearly indicates the notable influence of polymer-to-drug ratio and TPGS concentration on %DL. The final %DL model summary statistics (shown in Table 6.3) clearly produced the higher adjusted R^2 and predicted R^2 values obtained by quadratic model. A 3D surface plot for the influence of SA-F127-to-GLN ratio and concentration of TPGS on %DL are presented in Figure 6.3(c). The positive coefficient of mixed SA-F127 and TPGS indicated that the binary mixture of both the polymers have much better effect on %DL. It's because the mixed micelles of SA-F127 and TPGS have a larger hydrophobic core than the micelles of SA-F127 and TPGS alone. Such a better lipophilic core attracted the lipophilic GLN drug, which favours maximum %DL.

6.3.3.4 The effect of studied variable on %EE of GLN-PMM system

The %EE of polymeric micelles can also be utilized as the primary measures of the miscibility between drug molecules and polymers applied as the nanovehicles. The following quadratic regression 2nd order equations of the fitted model were used to maximize %EE:

$$\%EE = 66.54 - 21.68 \times A - 19.32 \times B + 1.043 \times AB - 10.92 \times A^2 - 3.984 \times B^2 \quad \ldots\ldots\ldots\ldots(6)$$

The SA-F127-to-GLN ratio and TPGS amount had a notable quadratic effect on EE% as per the ANOVA analysis. Increasing both the SA-F127-to-GLN ratio and TPGS concentration resulted in a substantial increase in EE%. As per the final %EE model statistics, the quadratic model also obtained the higher adjusted and predicted R^2. Figure 6.3(d) displays a 3D surface plot for the influence of SA-F127-to-GLN ratio and concentration of TPGS on %EE. It was examined that a low SA-F127-to-GLN ratio resulted in noticeable drug precipitation and a reduced EE%. The precipitation of drug might be caused by drug saturation at the inner core sites of the micelles. It is understood that at low SA-F127-to-GLN ratio the drug amount was higher in compared to the amount of SA-F127. As a result, it may be predicted that mixed polymeric micelles may improve the %EE of

lipophilic drugs up to a certain point, after that the increasing the drug concentration and decreasing the SA-F127-to-GLN ratio resulted in the drug precipitation [45]. The GLN is supposed to have higher attraction towards the hydrophobic SA-F127 than the hydrophilic TPGS. It concludes that the interaction between GLN and the inner core of the mixed micelles is better in the presence of SA-F127-to-GLN ratio.

Table 6.3: Summarized statistical output of the CCD analysis of GLN-PMM system.

Response	**Y1 : Particle size**	**Y2: PDI**	**Y3: %DL**	**Y4: % EE**
Minimum	14.70	0.221	0.61	96.60
Maximum	275.7	1.00	8.64	12.30
Model	Quadratic	Quadratic	Quadratic	Quadratic
R^2	0.9885	0.9839	0.9815	0.9846
Adjusted R^2	0.9803	0.9725	0.9682	0.9736
Predicted R^2	0.9094	0.8579	0.8268	0.8861
Adequate Precision	36.45	28.08	29.83	34.09
Significant terms (p-value)	A(0.0012), B(<0.0001), AB(<0.0001), A^2(0.0005), B^2(<0.0001)	A(<0.0001), B(<0.0046), A^2(0.0002)	A(0.0007), B(0.0001), AB(0.0243), A^2(0.0001), B^2 (0.0454)	A(<0.0001), B(<0.0046), A^2(0.0002)

After applying the CCD model to particle size, PDI, %DL and %EE, the composition with the 35:1 SA-F127-to-GLN ratio and 1.63 %w/v TPGS concentration that had the highest desirability value was chosen as the optimized formulation.

Table 6.4: Predicted and observed responses of the optimized GLN-PMM system.

Dependent Variable	**Predicted**	**Observed**	**Bias**
Particle Size	71.61	67.86	±2.87
PDI	0.490	0.582	±0.054
% DL	2.159	2.556	±0.87
%EE	86.60	91.49	±6.85

6.3.4 Characterization of optimized PMM and GLN-PMM system

6.3.4.1 CMC

The CMC is an important factor that influences the stability of polymeric mixed micelles in-vitro and in-vivo investigations. In the plot of the intensity ratio (I_1/I_3) versus SA-F127:TPGS concentration shown in the Figure 6.4(a), the lower the polymer concentration, the better the intensity ratio was observed in a slightly increasing order, but it was extremely increased beyond a specific polymer concentration. The inflection point considered as the CMC of SA-F127:TPGS system was determined to be 3.15 x 10^{-5} %w/v. The CMC of individual SA-F127 was found as 8.66 x 10^{-6} %w/v and reported value of the TPGS was 0.02 %w/v [46]. Here, the observed CMC of the mixed SA-F127:TPGS polymeric system found an intermediate value between the individual SA-F127 and TPGS polymers. This could be due to the fact that both polymers interacted well and had low CMC values. This mixed SA-F127:TPGS polymeric system's relatively low CMC value shows that their mixed polymeric micelles are very stable and can keep their shape even after being diluted a lot by the body fluids in the medium.

6.3.4.2 Particle size and morphological characterization

The average particle size as the D_h of PMM and GLN-PMM system was analyzed through the DLS technique and was found to be 58.8±4.08 nm and 67.00±2.07 nm, respectively. Figure 6.4(b) shows the size distribution curves of the examined mixed micelle formulations. The surface attributes of nanoscale vehicles are important because they influence the interaction with the microenvironment, which is determined by a combination of size and surface characteristics. Shen et al. [25] reported the D_h of the mixed micelles of the F127 and TPGS micelle system was 27.41±4.90 nm. The increases in the D_h of both PMM and GLN-PMM micelles in comparison to the F127:TPGS micelles was due to the conjugation of SA. Here, SA increases the D_h of the system but at the same time helps with more GLN encapsulation. The PMM and GLN-PMM micelles formulations had PDI values of 0.4312±0.08 and 0.5275 ±0.04, respectively. The PDI of the micelle formulations studied suggesting a low polydisperse particle population.

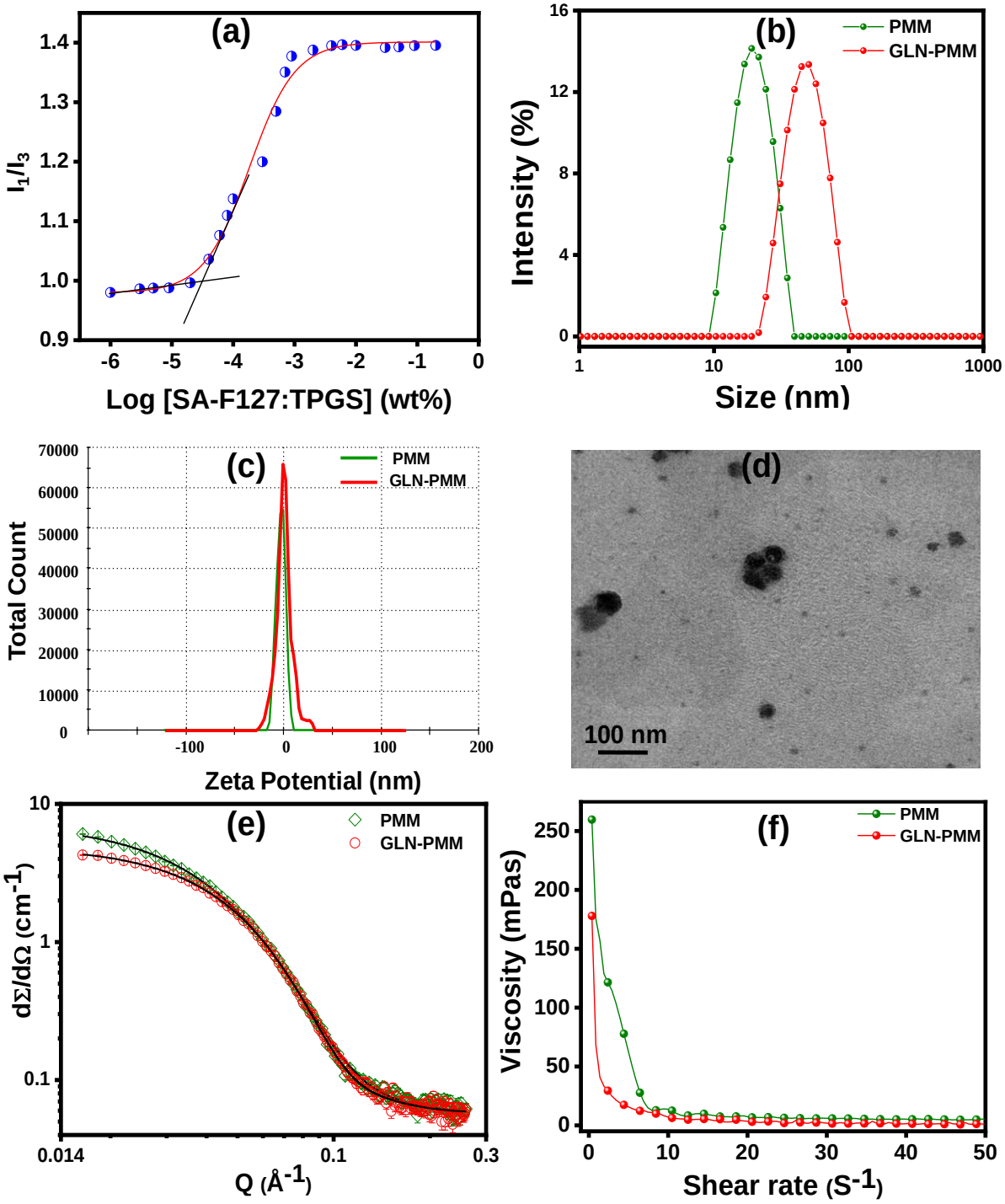

Figure 6.4: (a) Plot of (I_1/I_3) versus logarithmic concentration of optimized SA-F127:TPGS micellar system, **(b)** Micelles size distribution curves of optimized PMM and GLN-PMM system, **(c)** Zeta potential graphs of optimized PMM and GLN-PMM system, (**d)** TEM image of GLN-PMM system, **(e)** SANS profile of optimized PMM and GLN-PMM system, and **(f)** Rheological behavior optimized PMM and GLN-PMM system

The zeta potential of the particles has a high impact on the stability of a mixed micelle formulation. The PMM and GLN-PMM had zeta potential values of -1.62±0.23 mV and -3.85±1.39 mV, respectively [Figure 6.4(c)]. The negative zeta potential shows that the PMM and GLN-PMM systems are more dynamically stable. The SA-F127 and TPGS was nonionic and give slightly negative zeta potential, which indicate that the negative zeta potential mainly come from the presence of the pure drug molecules [47].

The GLN-PMM system was characterized by TEM and exhibited a particle size of ~50 nm. The TEM micrograph presented in Figure 6.4(d) confirmed the spherical shape of GLN-PMM. The large gap between adjacent micellar particles was observed in GLN-PMM, resulting from steric hindrance and electrostatic repulsion.

SANS is a unique approach for analyzing interdependent interactions between micelles and drugs. Figure 6.4(e) depicts the distribution curves from the SANS investigation of the PMM and GLN-PMM systems at 30±0.5°C. The various micellar parameters given by SANS are presented in Table 6.5. The micelle core radius (R_c) of PMM and GLN-PMM was 63.3 Å and 63.5 Å, respectively. The mixed nanomicelles showed very close scattering intensities in the SANS curve. Despite the fact that GLN molecules are incorporated into GLN-PMM micelles, the number density of the micelles has not changed much. It meant that the number of drug molecules in the mixed polymeric micelles was not much affect the micellar core. The morphology of PMM and GLN-PMM systems was found to have a spherical shape. The SANS results are in reasonable agreement with DLS and TEM measurements.

Table 6.5: Various SANS fitting parameters of PMM and GLN-PMM system.

Sample Code	Core radius R_c (Å)	*Aggregation number* (N_{agg})		
		SA-F127	TPGS	GLN
PMM	38.7 ± 0.3	1	249	—
GLN-PMM	38.0 ± 0.3	1	228	15

The optimal PMM and GLN-PMM viscosity measurements were performed at various shear rates. They are shown in Figure 6.4(f). The viscosity of the GLN-PMM system was lower than that of the PMM system. This reduction was only detected when the shear rate was minimal. This could be owing to the bonding that occurred during the encapsulation

of the GLN drug with PMM system. Beyond a particular shear rate, the viscosity of each of the samples was nearly constant.

6.3.4.3 Solid state characterization

The FTIR spectra of pure GLN, PMM, and GLN-PMM are displayed in Figure 6.5 (a). The IR spectra of pure GLN exhibited peaks at 3238.12 cm^{-1} (-NH stretching), 2936.78 cm^{-1} (C-H stretching), 1700.16 cm^{-1} (C=O stretching), 1650.89 cm^{-1} (-CONH- stretching), 1577.92 cm^{-1} (C=C aromatic stretching), 1453 cm^{-1} (C-H aromatic bending), and 1337.27 and 1167.61 cm^{-1} (O=S=O). The PMM spectra displayed two major peaks at 1212 cm^{-1} and 2971 cm^{-1} corresponding to C-O-C stretching and the -C-H stretching of the aliphatic chain, respectively. The absence of a prominent GLN peak in GLN-PMM indicates that the GLN drug is incorporated into the inner core of the mixed polymeric micelles, which indicated the existence of intermolecular interaction between the drug and the copolymers. Hence, this FTIR analysis reveals the physical interactions of GLN with mixed micelles and its compatibility with the core of PMM mixed micelles.

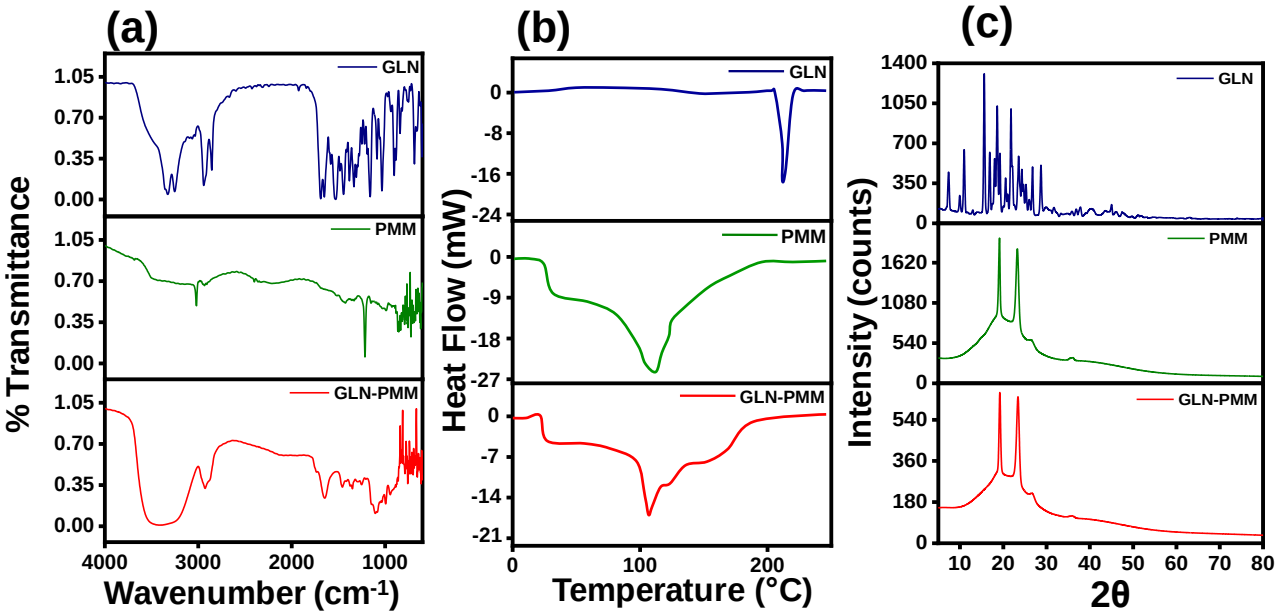

Figure 6.5 (a) FTIR spectrums, **(b)** DSC thermograms, and **(c)** XRD profiles of pure GLN, PMM, and GLN-PMM system.

The DSC analysis of pure GLN, PMM, and GLN-PMM is shown in Figure 6.5(b). DSC analysis has been used to determine the physical state of molecules and to investigate

any changes in the crystal properties of GLN during the formulation process. The sharp prominent endothermic peak at 215ºC for GLN was observed. The PMM showed a peak at 107.85°C, specifying to the relaxation peak of the glass transition. No distinct peak of any melting of an individual polymer was found in the case of PMM. The GLN-PMM curve was somewhat similar to PMM with a reduction in intensity and did not detect any peak at near 215ºC, the melting point of GLN. The disappearance of the GLN distinctive melting endothermic peak indicates that GLN has been incorporated into the core of mixed polymeric micelles. As a result, it was proven that GLN was present in the GLN-PMM system in a non-crystalline or amorphous nature.

Figure 6.5(c) shows a comparison of the XRD patterns of GLN, PMM, and GLN-PMM systems. GLN displays high intensity and clear crystalline peaks between 10° and 30° (2θ) regions, indicating that it is highly crystalline in nature. The presence of only two intense peaks in the XRD pattern of the PMM at 2θ angles of 19.20° and 23.20° suggested the non-crystalline nature of the PMM. Similar to the PMM, the optimized GLN-PMM had the same peaks with decreases intensity and flat patterns, indicating the typical non-crystalline nature of the formulation. The intensity of the peak is actually directly proportional to the crystalline form of the system. The GLN-PMM showed a common amorphous pattern with a total absence of the number of classified peaks of GLN, conferming that GLN was molecularly solubilized in a non-crystalline state in the mixed micelles [48]. This proved that the GLN was encapsulated in the PMM micelles. As a result, the solubility, percentage of release, and speed of dissolution were all improved, which are all good qualities for a drug delivery vehicle.

6.3.5 Location of GLN solubilization in GLN-PMM system

The location of GLN in the GLN-PMM mixed micellar system was assessed using ^{1}H NMR technique, which is a non-invasive method [49]. Figure 6.6(a) shows the NMR spectrum of pure GLN in $CDCl_3$. The spectrum of GLN clearly showed the δ at 6.49-6.51 (primary -$CONH_2$), 7.42–7.88 (aromatic benzene ring), 8.20-8.38 (secondary –$CONH_2$), and 9.286-9.289 (-CH of pyrazine) ppm. The spectrums of the PMM and GLN-PMM in D_2O (Figure 6.6(b) & 6.6(c)) displayed almost similar signals of protons.

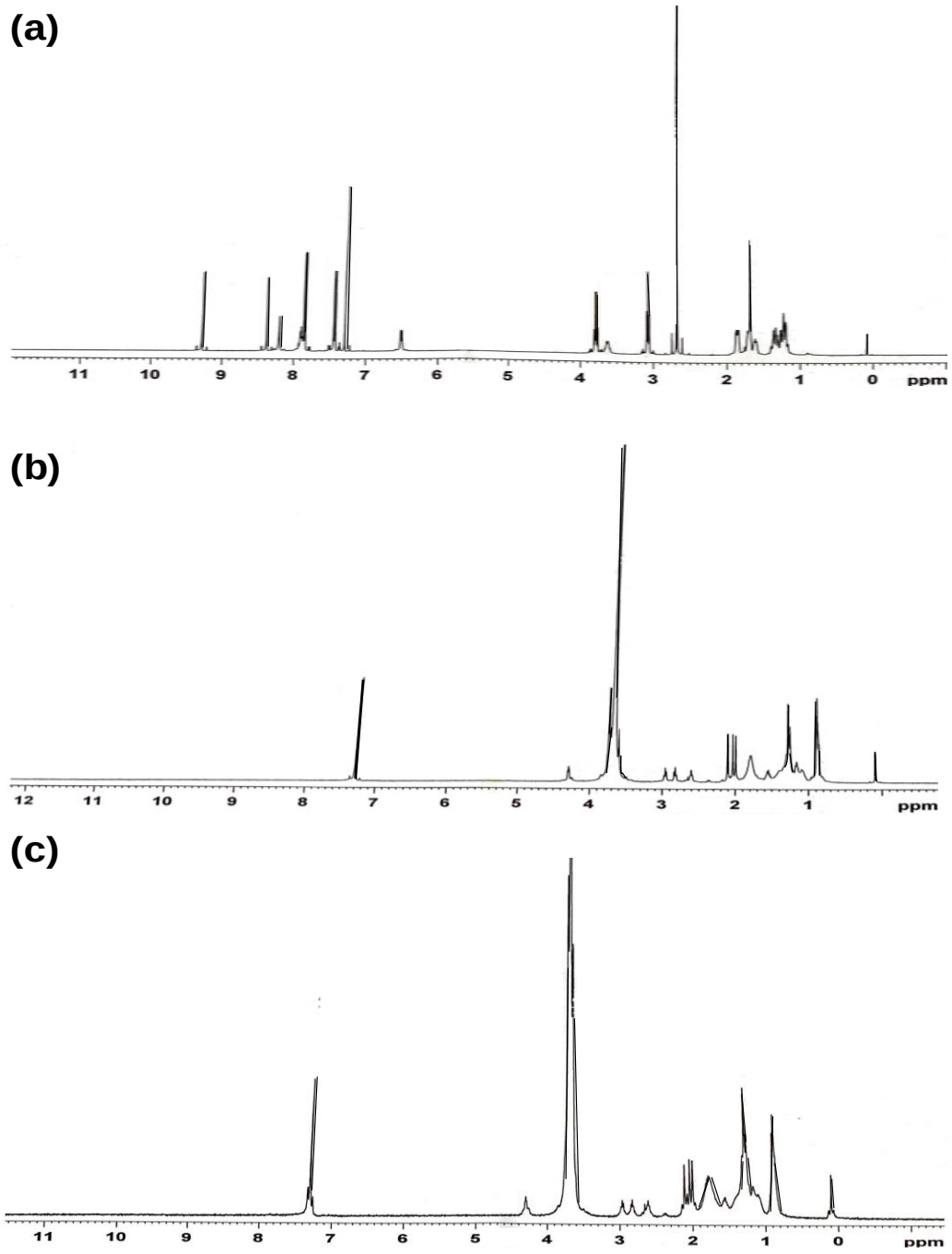

Figure 6.6: ^{1}H NMR spectra of **(a)** GLN in $CDCl_3$, **(b)** PMM system in D_2O and **(c)** GLN-PMM system in D_2O.

The signals of TPGS were also found (δ= 7.298 ppm, aromatic ring signal of TPGS) in both the spectrum. Here, the peaks of the GLN are absent in the spectrum of GLN-PMM system. Moreover, three signals of the PPO at 0.90-0.88(CH_3), 3.64 (CH), and 3.67-3.74

(CH_2) GLN-PMM showed the upfield shift of PPO of 0.01 ppm in comparison to PMM. A downfield or upfield shift is dependent on the polar or nonpolar surrounding environment in the medium. A shift of copolymer protons shows the location of drug solubilization [50]. These results clearly confirmed that GLN was successfully placed into the inner core of mixed PMM micelles.

6.3.6 Stability study

Stability studies of formulations are vital for daily use as well as thinking about industrial production. To grant a long shelf-life on the GLN-PMM system, it one portion was stored at RT and another portion store under refrigerated conditions (2°-8°C) for three months (Figure 6.7). At both temperatures, the lyophilized GLN-PMM was stable. Here, GLN-PMM system can cause a slight increment in particle size because of nucleation or possible aggregation of micelles.

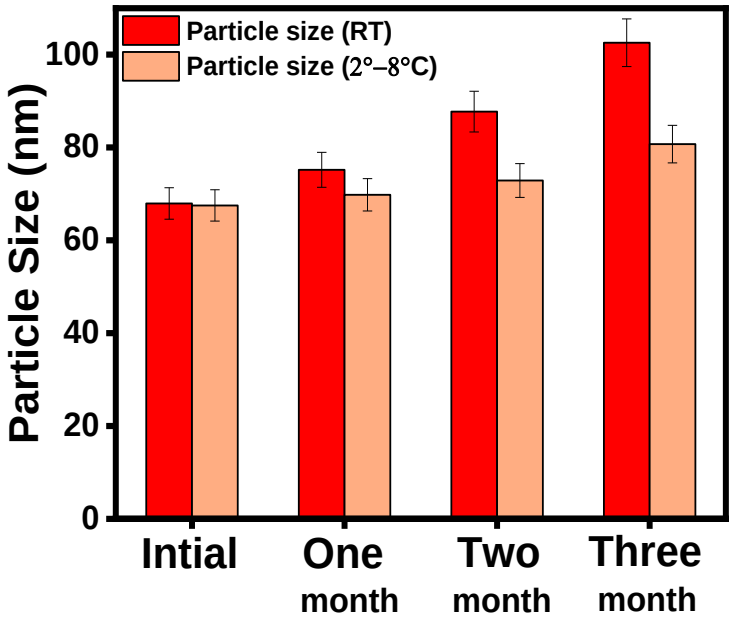

Figure 6.7: Storage stability of optimized GLN-PMM system at RT and refrigerated temperature (2°-8°C)

6.3.7 Biological Investigation

6.3.7.1 In-vitro Drug release profile

In-vitro drug release of GLN from the mixed GLN-PMM micelles was studied by using the dialysis membrane bag method at three different pH. The GLN release was carried out for 24 hrs as shown in Figure 6.8**.** Here it was seen that 75.34 ± 1.09 % of GLN was released from the GLN-PMM at pH = 1.2, while 90.24 ± 1.45 % GLN was released at pH = 6.8, and 99.19±2.26% GLN was released at pH = 7.4. GLN dissolution profiles were greatly influenced by its solubility. The solubility of drug increased gradually with pH until it reached pKa at it again increased dramatically. As a result, it indicated that GLN was released from any formulations with a slow dissolution rate at below pH 6.0, with less than 40% of the entire amount dissolving [51].

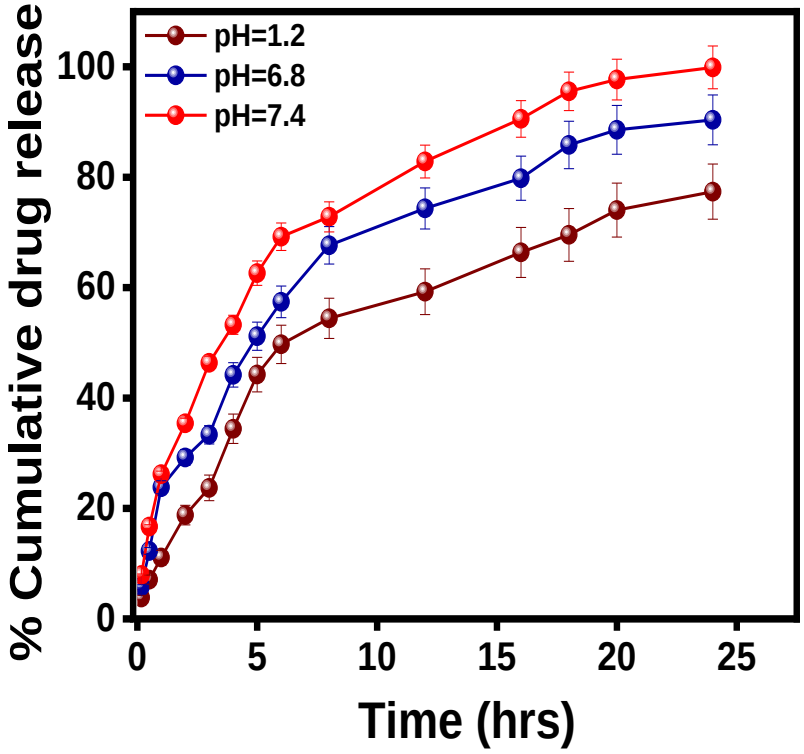

Figure 6.8: *In-vitro* release profile of optimized GLN-PMM system in different pH at 37°±0.5°C.

Table 6.6: Regression coefficient of drug release models in various pH environments at 37±0.5°C.

Release kinetic model	*Regression coefficient (R^2)*		
	pH= 1.2	**pH=6.8**	**pH= 7.4**
0^{th} order	0.8543	0.8666	0.8390
1^{st} order	0.9042	0.7879	0.8102
Higuchi	0.9535	**0.9826**	**0.9971**
Korsmeyer-Peppas	**0.9907**	0.9745	0.9944

The results of *in-vitro* drug release studies were evaluated using different release kinetic models. From Table 6.6**,** the regression coefficient of the Korsmeyer-Peppas for the GLN-PMM system was 0.9907, which was greater than other models for the GLN release at pH 1.2. Similarly, the regression coefficient of the Higuchi model for GLN release was found to be 0.9826. It was greater than other models for the release of at pH 6.8. Also, the regression coefficient of the Higuchi model for GLN release was found to be 0.9971 at pH 7.4.

6.3.7.2 Ex-vivo permeation study

An *ex-vivo* permeation study was done through a Franz diffusion cell (with a 2.5 cm diameter and 5.722 cm^2 area). As shown in Figure 6.9(a), the ex-vivo drug permeation from a pure GLN suspension showed that nearly 36.08 ±1.09 % of the drug was permeated from the intestine, whereas from a GLN-PMM system, 88.86 ± 3.39 % of the GLN was permeated. An increase in permeation by mixed micellar formulation may be resulted due to the small particle size and slightly negative zeta potential of the GLN-PMM. Because of the entrapment of drugs inside the core of mixed micelles, the release of drugs was sustained. The regression coefficient of the plot of the Higuchi model for mixed micelles was found to be 0.9608, which was higher than any other fitted model (Table 6.7**).**

Table 6.7: Regression coefficient ($R^{2)}$ values for *ex-vivo* drug permeability study

Kinetic model	GLN	GLN-PMM
0^{th} order	**0.9831**	0.8553
1^{st} order	0.5654	0.5916
Higuchi	0.9012	**0.9608**
Korsmeyer-Peppas	0.8936	0.9457

6.3.7.3 In-vivo anti-diabetic study

Blood glucose level estimated in healthy normal rats at different time point is shown in Figure 6.9(b). Before administration of diabetes in rats the blood glucose level was 119.51±6.75 mg/dL. After administration of diabetes in rats the blood glucose level of 217.6±8.56 mg/dL was observed. The optimized GLN-PMM system is compared with the marketed formulation. When optimized GLN-PMM and marketed formulation were administered in rats, the reduction in blood glucose levels was normal within 2 hrs. The blood glucose level of marketed formulation and GLN-PMM were 143±5.89 mg/dL and 118.50±4.81 mg/dL respectively whereas after 24 hrs the blood glucose level of marketed formulation and GLN-PMM were 138.67±3.50 mg/dL and 114.36±7.45 mg/dL, respectively. Results indicate the blood glucose level sustained for studied period. The optimized GLN-PMM reduced more blood glucose level in rats compared to the marketed formulation. These results clearly indicated that because of enhanced solubility and dissolution rate of GLN in the GLN-PMM formulation improved the bioavailability of GLN. Therefore, the fabricated optimized GLN-PMM micellar system has enhancing drug potential upon drug permeability.

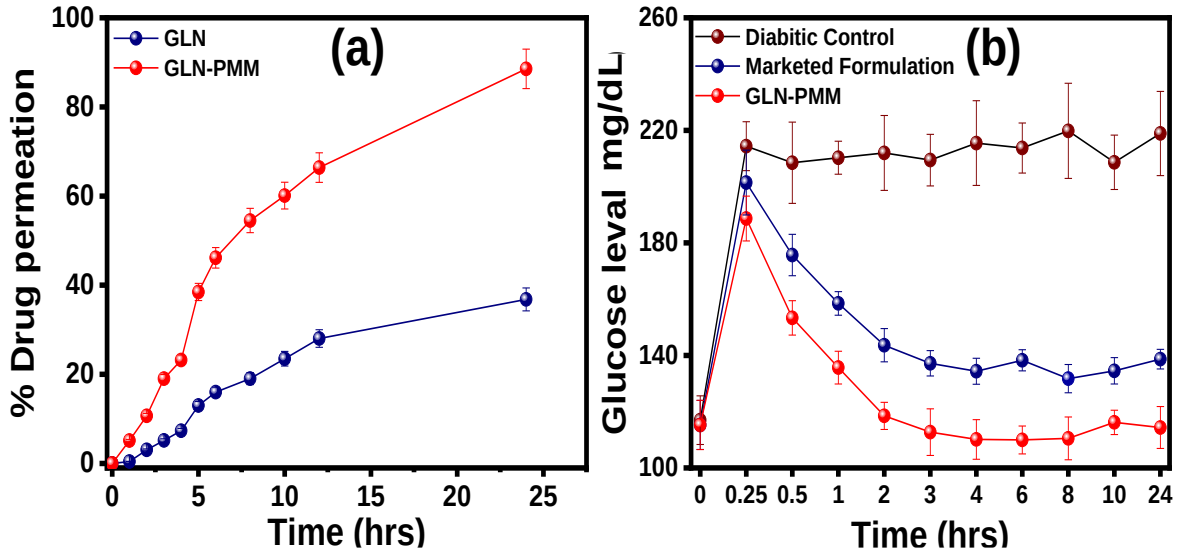

Figure 6.9: (a) *Ex-vivo* permeation study of GLN and GLN-PMM system and **(b)** *In-vivo* anti-diabetic study of diabetic control, marketed formulation and GLN-PMM system.

6.4: References

[1] H. Grohganz, P.A. Priemel, K. Löbmann, L.H. Nielsen, R. Laitinen, A. Mullertz, G. Van den Mooter, T. Rades, Refining stability and dissolution rate of amorphous drug formulations, Expert Opin. Drug Deliv. 11 (2014) 977–989.

[2] K. Noh, B.S. Shin, K. Kwon, H. Yun, E. Kim, T.C. Jeong, W. Kang, Absolute bioavailability and metabolism of aceclofenac in rats, Arch. Pharm. Res. 38 (2015) 68–72.

[3] C.J.H. Porter, N.L. Trevaskis, W.N. Charman, Lipids and lipid-based formulations: optimizing the oral delivery of lipophilic drugs, Nat. Rev. Drug Discov. 6 (2007) 231–248.

[4] B. Morakul, J. Suksiriworapong, M.T. Chomnawang, P. Langguth, V.B. Junyaprasert, Dissolution enhancement and in vitro performance of clarithromycin nanocrystals produced by precipitation–lyophilization–homogenization method, Eur. J. Pharm. Biopharm. 88 (2014) 886–896.

[5] S. Kumar, R. Jog, J. Shen, B. Zolnik, N. Sadrieh, D.J. Burgess, In vitro and in vivo performance of different sized spray-dried crystalline itraconazole, J. Pharm. Sci. 104 (2015) 3018–3028.

[6] H. Li, L. Dong, Y. Liu, G. Wang, G. Wang, Y. Qiao, Biopharmaceutics classification of puerarin and comparison of perfusion approaches in rats, Int. J. Pharm. 466 (2014) 133–138.

[7] X. Zhang, Y. Wu, Y. Hong, X. Zhu, L. Lin, Q. Lin, Preparation and evaluation of dl-praeruptorin A microemulsion based hydrogel for dermal delivery, Drug Deliv. 22 (2015) 757–764.

[8] Z. Fatfat, M. Fatfat, H. Gali-Muhtasib, Micelles as potential drug delivery systems for colorectal cancer treatment., World J. Gastroenterol. 28 (2022) 2867.

[9] D. V Bhalani, B. Nutan, A. Kumar, A.K. Singh Chandel, Bioavailability Enhancement Techniques for Poorly Aqueous Soluble Drugs and Therapeutics, Biomedicines. 10 (2022) 2055.

[10] M. Ghezzi, S. Pescina, C. Padula, P. Santi, E. Del Favero, L. Cantù, S. Nicoli, Polymeric micelles in drug delivery: An insight of the techniques for their

characterization and assessment in biorelevant conditions, J. Control. Release. 332 (2021) 312–336.

[11] F.U. Vaidya, R. Sharma, S. Shaikh, D. Ray, V.K. Aswal, C. Pathak, Pluronic micelles encapsulated curcumin manifests apoptotic cell death and inhibits pro-inflammatory cytokines in human breast adenocarcinoma cells, Cancer Rep. 2 (2019) e1133.

[12] I. Jarak, C.L. Varela, E.T. da Silva, F.F.M. Roleira, F. Veiga, A. Figueiras, Pluronic-based nanovehicles: Recent advances in anticancer therapeutic applications, Eur. J. Med. Chem. 206 (2020) 112526.

[13] M. Khimani, H. Patel, V. Patel, P. Parekh, R.L. Vekariya, Self-assembly of stimuli-responsive block copolymers in aqueous solutions: An overview, Polym. Bull. 77 (2020) 5783–5810.

[14] A. Patra, A.K. Shenoy, J.A. Bush, M. Kazi, M.D. Hussain, S. Satpathy, A.K. Shenoy, J.A. Bush, M. Kazi, M.D. Hussain, Formulation and evaluation of mixed polymeric micelles of quercetin for treatment of breast, ovarian, and multidrug resistant cancers, Int. J. Nanomedicine. 13 (2018) 2869.

[15] H. Hu, A. Petrosyan, N.A. Osna, T. Liu, A.A. Olou, D.Y. Alakhova, P.K. Singh, A. V Kabanov, E.A. Faber Jr, T.K. Bronich, Pluronic block copolymers enhance the anti-myeloma activity of proteasome inhibitors, J. Control. Release. 306 (2019) 149–164.

[16] R.K. Sharma, S. Shaikh, D. Ray, V.K. Aswal, Binary mixed micellar systems of PEO-PPO-PEO block copolymers for lamotrigine solubilization: a comparative study with hydrophobic and hydrophilic copolymer, J. Polym. Res. 25 (2018) 1–11.

[17] M.J. Barthel, F.H. Schacher, U.S. Schubert, Poly (ethylene oxide)(PEO)-based ABC triblock terpolymers–synthetic complexity vs. application benefits, Polym. Chem. 5 (2014) 2647–2662.

[18] S.J. Shaikh, H.S. Patel, D. Ray, V.K. Aswal, S. Singh, R. Vijayvargia, U. Sheth, R.K. Sharma, Enhanced Solubility and Oral Bioavailability of Hydrophobic Drugs Using Pluronic Nanomicelles: An In-Vitro Evaluation, ChemistrySelect. 6 (2021) 7040-7048.

[19] R.N. Shamma, R.H. Sayed, H. Madry, N.S. El Sayed, M. Cucchiarini, Triblock Copolymer Bioinks in Hydrogel Three-Dimensional Printing for Regenerative Medicine: A Focus on Pluronic F127, Tissue Eng. Part B Rev. 28 (2022) 451–463.

[20] M.S.H. Akash, K. Rehman, S. Chen, Pluronic F127-based thermosensitive gels for

delivery of therapeutic proteins and peptides, Polym. Rev. 54 (2014) 573–597.

[21] B. Shriky, A. Kelly, M. Isreb, M. Babenko, N. Mahmoudi, S. Rogers, O. Shebanova, T. Snow, T. Gough, Pluronic F127 thermosensitive injectable smart hydrogels for controlled drug delivery system development, J. Colloid Interface Sci. 565 (2020) 119–130.

[22] M.A. Grimaudo, S. Pescina, C. Padula, P. Santi, A. Concheiro, C. Alvarez-Lorenzo, S. Nicoli, Poloxamer 407/TPGS mixed micelles as promising carriers for cyclosporine ocular delivery, Mol. Pharm. 15 (2018) 571–584.

[23] M. Cagel, E. Bernabeu, L. Gonzalez, E. Lagomarsino, M. Zubillaga, M.A. Moretton, D.A. Chiappetta, Biomedicine & Pharmacotherapy Mixed micelles for encapsulation of doxorubicin with enhanced in vitro cytotoxicity on breast and ovarian cancer cell lines versus Doxil ®, Biomed. Pharmacother. 95 (2017) 894–903.

[24] X. Meng, J. Liu, X. Yu, J. Li, X. Lu, T. Shen, Pluronic F127 and D-α-tocopheryl polyethylene glycol succinate (TPGS) mixed micelles for targeting drug delivery across the blood brain barrier, Sci. Rep. 7 (2017) 1–12.

[25] C. Shen, J. Zhu, J. Song, J. Wang, B. Shen, H. Yuan, X. Li, Formulation of pluronic F127/TPGS mixed micelles to improve the oral absorption of glycyrrhizic acid, Drug Dev. Ind. Pharm. 1080 (2020) 1775634.

[26] S. Rathod, P. Bahadur, S. Tiwari, Nanocarriers based on vitamin E-TPGS: Design principle and molecular insights into improving the efficacy of anticancer drugs, Int. J. Pharm. 592 (2021) 120045.

[27] M.T. Luiz, L.D. Di Filippo, R.C. Alves, V.H.S. Araújo, J.L. Duarte, J.M. Marchetti, M. Chorilli, The use of TPGS in drug delivery systems to overcome biological barriers, Eur. Polym. J. 142 (2021) 110129.

[28] H. Yan, X. Du, R. Wang, G. Zhai, Progress in the study of D-α-tocopherol polyethylene glycol 1000 succinate (TPGS) reversing multidrug resistance, Colloids Surfaces B Biointerfaces. 205 (2021) 111914.

[29] A.M. Butt, M.C.I.M. Amin, H. Katas, N. Sarisuta, W. Witoonsaridsilp, R. Benjakul, In vitro characterization of pluronic F127 and D--tocopheryl polyethylene glycol 1000 succinate mixed micelles as nanocarriers for targeted anticancer-drug delivery, J. Nanomater. 2012 (2012).

[30] P.K. Sharma, S.R. Bhatia, Effect of anti-inflammatories on Pluronic® F127: micellar assembly, gelation and partitioning, Int. J. Pharm. 278 (2004) 361–377.

[31] Y. Zhang, Y.M. Lam, Controlled synthesis and association behavior of graft Pluronic in aqueous solutions, J. Colloid Interface Sci. 306 (2007) 398–404.

[32] S. Tiwari, V. Kansara, P. Bahadur, Targeting Anticancer Drugs with Pluronic Aggregates: Recent Updates, Int. J. Pharm. 586 (2020) 119544.

[33] P. Singla, S. Garg, J. McClements, O. Jamieson, M. Peeters, R.K. Mahajan, Advances in the therapeutic delivery and applications of functionalized Pluronics: A critical review, Adv. Colloid Interface Sci. 299 (2022) 102563.

[34] G. Bruni, I. Ghione, V. Berbenni, A. Cardini, D. Capsoni, A. Girella, C. Milanese, A. Marini, The Physico-Chemical Properties of Glipizide: New Findings, Molecules. 26 (2021) 3142.

[35] J. Joya-Galeana, M. Fernandez, A. Cervera, S. Reyna, S. Ghosh, C. Triplitt, N. Musi, R.A. DeFronzo, E. Cersosimo, Effects of insulin and oral anti-diabetic agents on glucose metabolism, vascular dysfunction and skeletal muscle inflammation in type 2 diabetic subjects, Diabetes. Metab. Res. Rev. 27 (2011) 373–382.

[36] R.K. Verma, S. Garg, Selection of excipients for extended release formulations of glipizide through drug–excipient compatibility testing, J. Pharm. Biomed. Anal. 38 (2005) 633–644.

[37] L. Groop, R. Defronzo, L. Luzi, A. Melander, Hyperglycaemia and absorption of sulphonylurea drugs, Lancet. 334 (1989) 129–130.

[38] A.M. Aly, M.K. Qato, M.O. Ahmad, Enhancement of the dissolution rate and bioavailability of glipizide through cyclodextrin inclusion complex, Pharm. Technol. 27 (2003) 54.

[39] S.S. Kushare, S.G. Gattani, Microwave-generated bionanocomposites for solubility and dissolution enhancement of poorly water-soluble drug glipizide: in-vitro and in-vivo studies, J. Pharm. Pharmacol. 65 (2013) 79–93.

[40] Q. Gao, Q. Liang, F. Yu, J. Xu, Q. Zhao, B. Sun, Synthesis and characterization of novel amphiphilic copolymer stearic acid-coupled F127 nanoparticles for nano-technology based drug delivery system, Colloids Surfaces B Biointerfaces. 88 (2011) 741–748.

[41] R.N. Dash, H. Mohammed, T. Humaira, D. Ramesh, Design, optimization and evaluation of glipizide solid self-nanoemulsifying drug delivery for enhanced solubility and dissolution, Saudi Pharm. J. 23 (2015) 528–540.

[42] S.S. Kulthe, N.N. Inamdar, Y.M. Choudhari, S.M. Shirolikar, L.C. Borde, V.K. Mourya, Mixed micelle formation with hydrophobic and hydrophilic Pluronic block copolymers: implications for controlled and targeted drug delivery, Colloids Surfaces B Biointerfaces. 88 (2011) 691–696.

[43] C. Rupp, H. Steckel, B.W. Müller, Solubilization of poorly water-soluble drugs by mixed micelles based on hydrogenated phosphatidylcholine, Int. J. Pharm. 395 (2010) 272–280.

[44] R. Zeisig, K. Shimada, S. Hirota, D. Arndt, Effect of sterical stabilization on macrophage uptake in vitro and on thickness of the fixed aqueous layer of liposomes made from alkylphosphocholines, Biochim. Biophys. Acta (BBA)-Biomembranes. 1285 (1996) 237–245.

[45] C.-F. Mu, P. Balakrishnan, F.D. Cui, Y.M. Yin, Y.B. Lee, H.G. Choi, C.S. Yong, S.J. Chung, C.K. Shim, D.D. Kim, The effects of mixed MPEG–PLA/Pluronic® copolymer micelles on the bioavailability and multidrug resistance of docetaxel, Biomaterials. 31 (2010) 2371–2379.

[46] H. Kulhari, D. Pooja, S. Shrivastava, S.R. Telukutala, A.K. Barui, C.R. Patra, G.M.N. Vegi, D.J. Adams, R. Sistla, Cyclic-RGDfK peptide conjugated succinoyl-TPGS nanomicelles for targeted delivery of docetaxel to integrin receptor over-expressing angiogenic tumours, Nanomedicine Nanotechnology, Biol. Med. 11 (2015) 1511–1520.

[47] L. Zhao, J. Du, Y. Duan, Y. Zang, H. Zhang, C. Yang, F. Cao, G. Zhai, Curcumin loaded mixed micelles composed of Pluronic P123 and F68: Preparation, optimization and in vitro characterization, Colloids Surfaces B Biointerfaces. 97 (2012) 101–108.

[48] S. Ji, X. Lin, E. Yu, C. Dian, X. Yan, L. Li, M. Zhang, W. Zhao, L. Dian, Curcumin-Loaded Mixed Micelles : Preparation , Characterization , and In Vitro Antitumor Activity, 2018 (2018).

[49] M.A. Adahoun, M.-A.H. Al-Akhras, M.S. Jaafar, M. Bououdina, Enhanced anti-cancer and antimicrobial activities of curcumin nanoparticles, Artif. Cells,

Nanomedicine, Biotechnol. 45 (2017) 98–107.

[50] P. Singla, S. Chabba, R.K. Mahajan, A systematic physicochemical investigation on solubilization and in vitro release of poorly water soluble oxcarbazepine drug in pluronic micelles, Colloids Surfaces A Physicochem. Eng. Asp. 504 (2016) 479–488.

[51] C. Zhao, C. Jin, H. Gao, L. Wang, H. Liu, Z. He, Effect of raw material variability of glipizide on the in vitro dissolution rate and in vivo bioavailability performance: The importance of particle size, Asian J. Pharm. Sci. 14 (2019) 165–173.